

# Supporting Information for "Source Parameters of S1222a Marsquake obtained from Spectral Analyses using Empirical Green's Function"

Taichi Kawamura<sup>1</sup>, Zongbo Xu<sup>1</sup>, Wanbo Xiao<sup>1</sup>, Ludovic Margerin<sup>2</sup>, Sabrina

Menina<sup>1</sup>, Philippe Lognonné<sup>1</sup>, William Bruce Banerdt<sup>3</sup>

<sup>1</sup>Université Paris Cité, Institut de physique du globe de Paris, CNRS, Paris, France

<sup>2</sup>Institut de Recherche en Astrophysique et Planétologie, Toulouse, France

<sup>3</sup>Jet Propulsion Laboratory, California Institute of Technology, CA, USA

## Contents of this file

1. Tables S1 to S2
2. Figures S1 to S11

---

**Table S1.** Events used for EGF analyses of S1094b<sup>a</sup>

Event Name	Event Type	Event Quality	Magnitude	ts-tp (s)
S1094	VF	A	4.0	342
S0218a	VF	B	2.5	336
S0387a	VF	B	2.1	347
S0424c	VF	B	2.2	338
S0869b	VF	B	2.5	330

<sup>a</sup> The first event of the table is the reference event.

**Table S2.** Events used for EGF analyses of S1222a<sup>b</sup>

Event Name	Event Type	Event Quality	Magnitude	ts-tp (s)
S1222a	BB	A	4.7	214
S1135c	HF	B	1.8	216
S1091a	HF	B	1.8	218
S1082c	HF	B	2.3	229
S1040b	HF	B	2.1	218
S1024c	HF	B	2.0	235
S0997a	HF	B	2.1	232
S0882a	VF	B	2.4	234
S0758a	HF	B	2.1	190
S0756a	VF	B	2.8	206
S0436c	HF	B	2.1	232
S0334a	VF	B	2.1	214
S0327c	HF	B	1.9	199
S0228c	HF	B	1.9	232
S0183a	LF	B	2.7	194

<sup>b</sup> The first event of the table is the reference event.

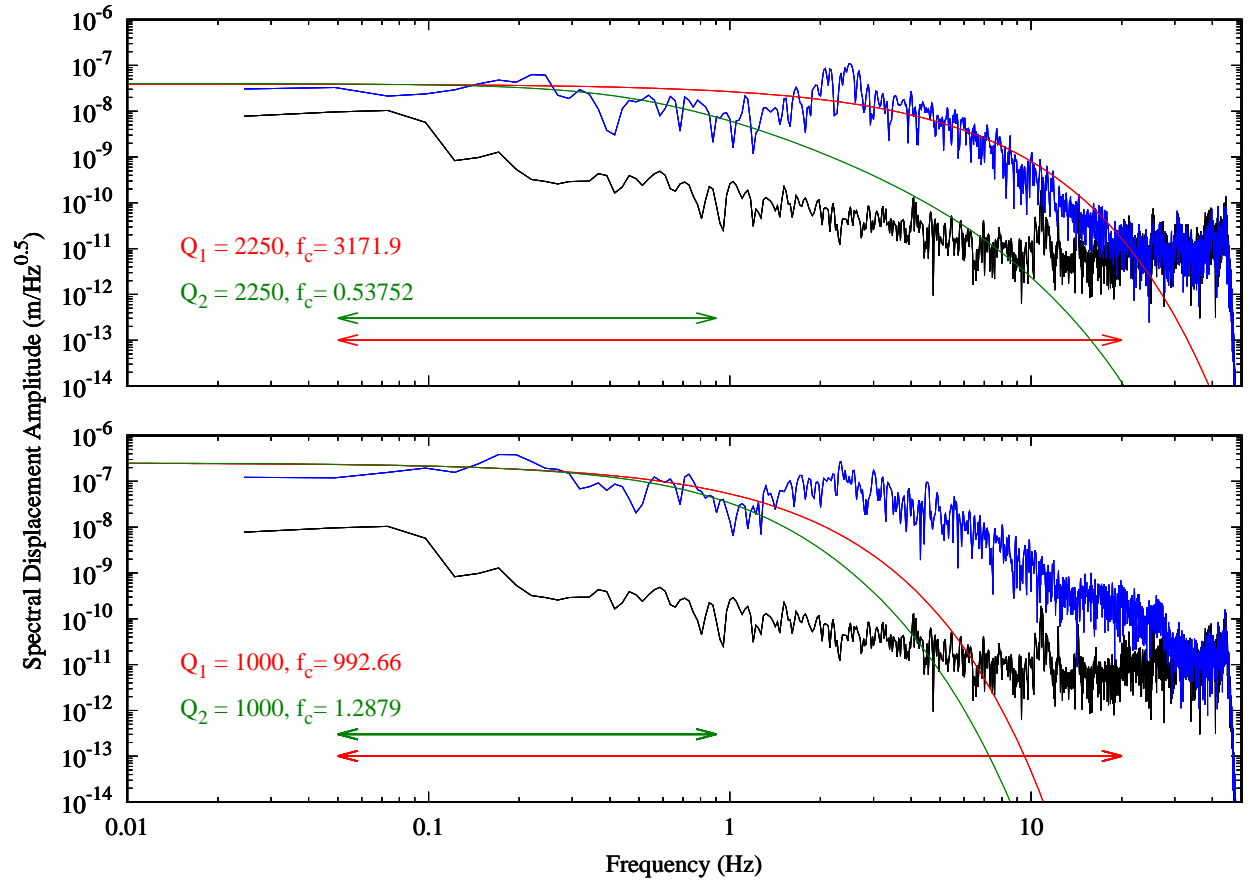


**Figure S1.** S1222a spectra for P and S waves. The top panel shows the P spectrum and the bottom panel shows the S spectrum. The seismic spectra are shown in blue and the noise spectra is shown in black. The red line is the fitting with Eq. ?? using reference  $Q$  values from (?, ?) and wide frequency band (0.05-20Hz; shown in red arrow)). The green line shows the result of the fitting with the narrow frequency band (0.05-0.9Hz; shown in green arrow).

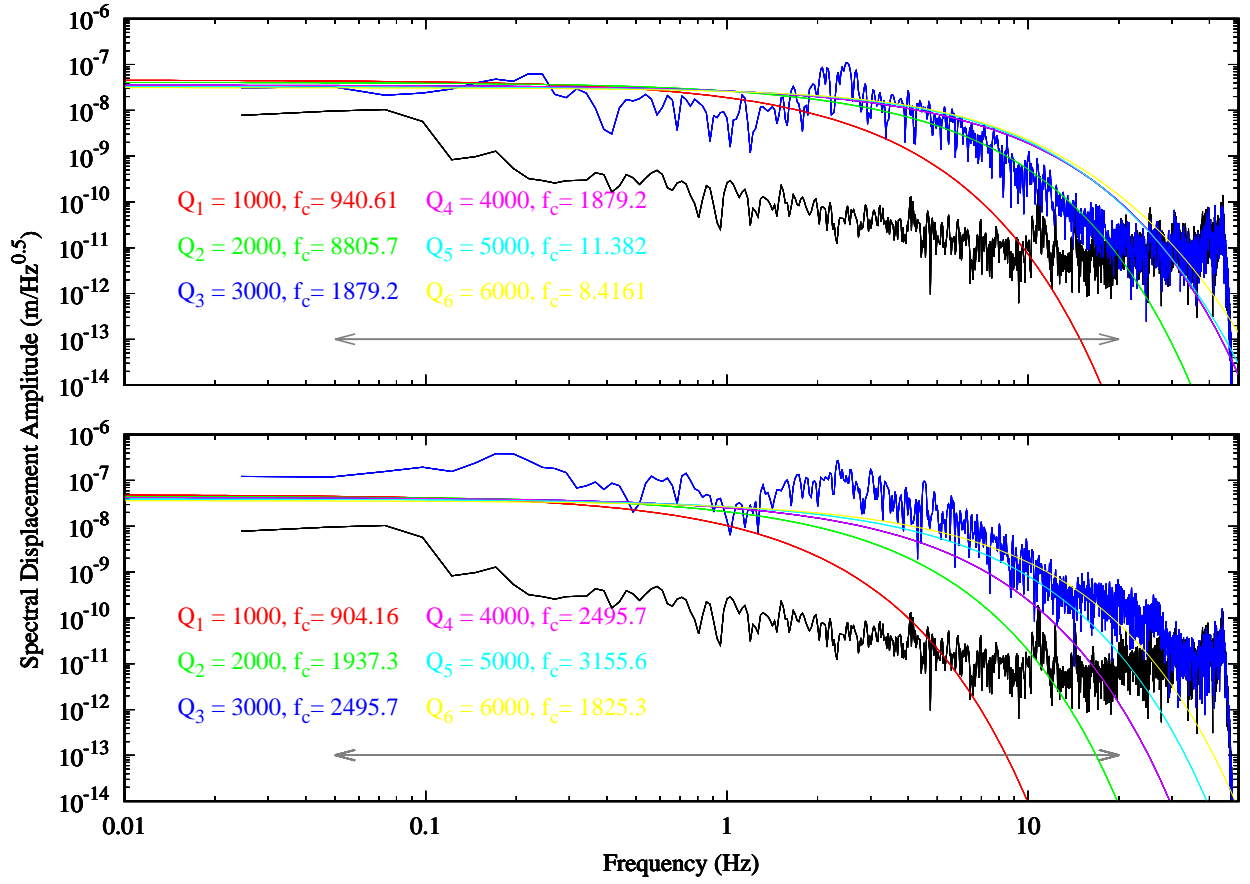


**Figure S2.** Results of Raw S1222a spectra fitted to  $\omega^2$  model with various Q factor. 0.05-20Hz was used to fit the model to the observation data. Even with the wide variety of  $Q$  that was used to explain the observations, we were not able to find a reasonable solution. For most of the cases, we found  $f_c$  extremely high and outside the frequency band we are using for the analyses. This implies that the decay of S1222a can be almost fully explained with attenuation, which is unreasonable following the former study which obtained  $f_c$  within the frequency band of the fit.

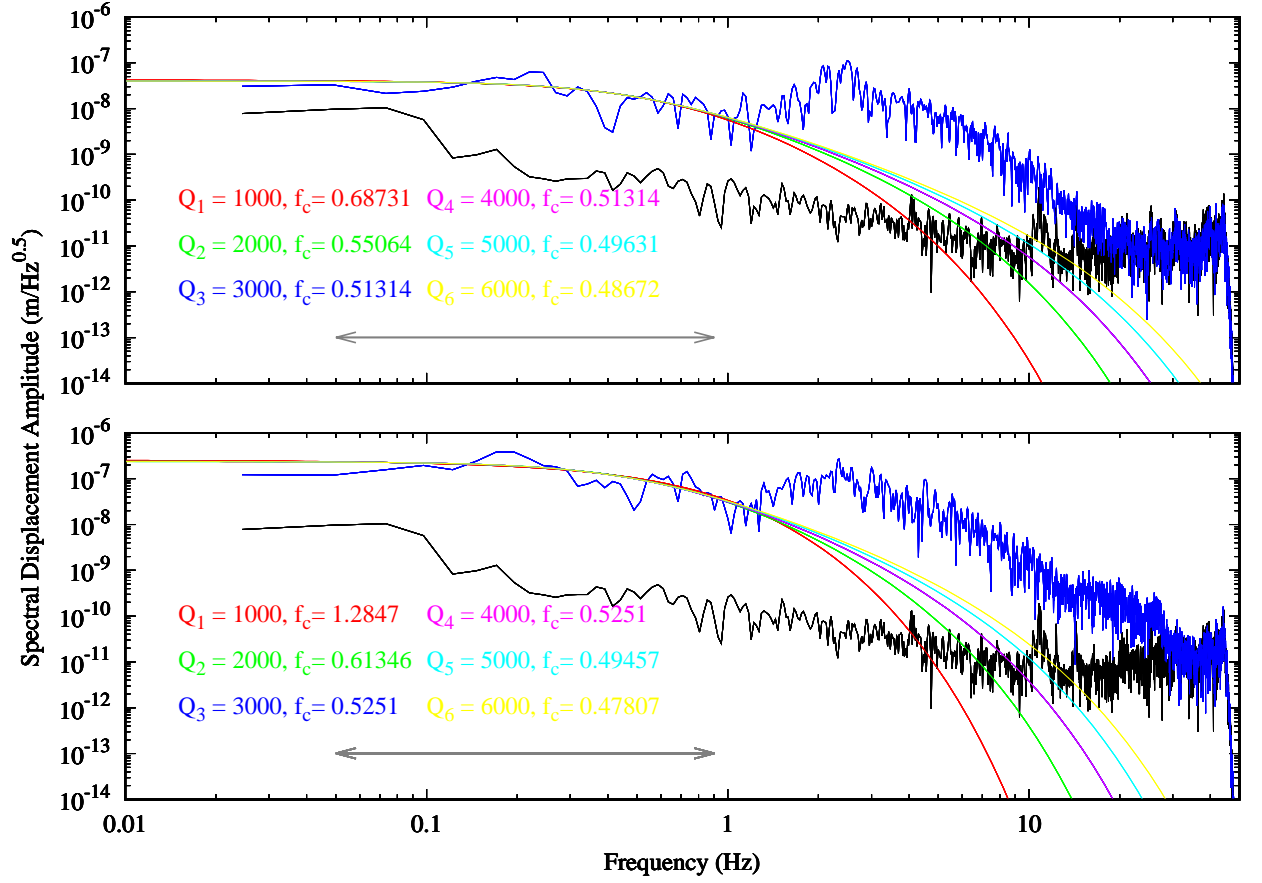


**Figure S3.** Results of Raw S1222a spectra fitted to  $\omega^2$  model with various Q factor. 0.05-8Hz was used to fit the model to the observation data. The obtained reasonable  $f_c$  for wide range of Q value. We found that the analyses suffer from the trade off between  $f_c$  and Q and since we excluded the high frequency portion of the spectra, we were not able to resolve the difference between different Q values.

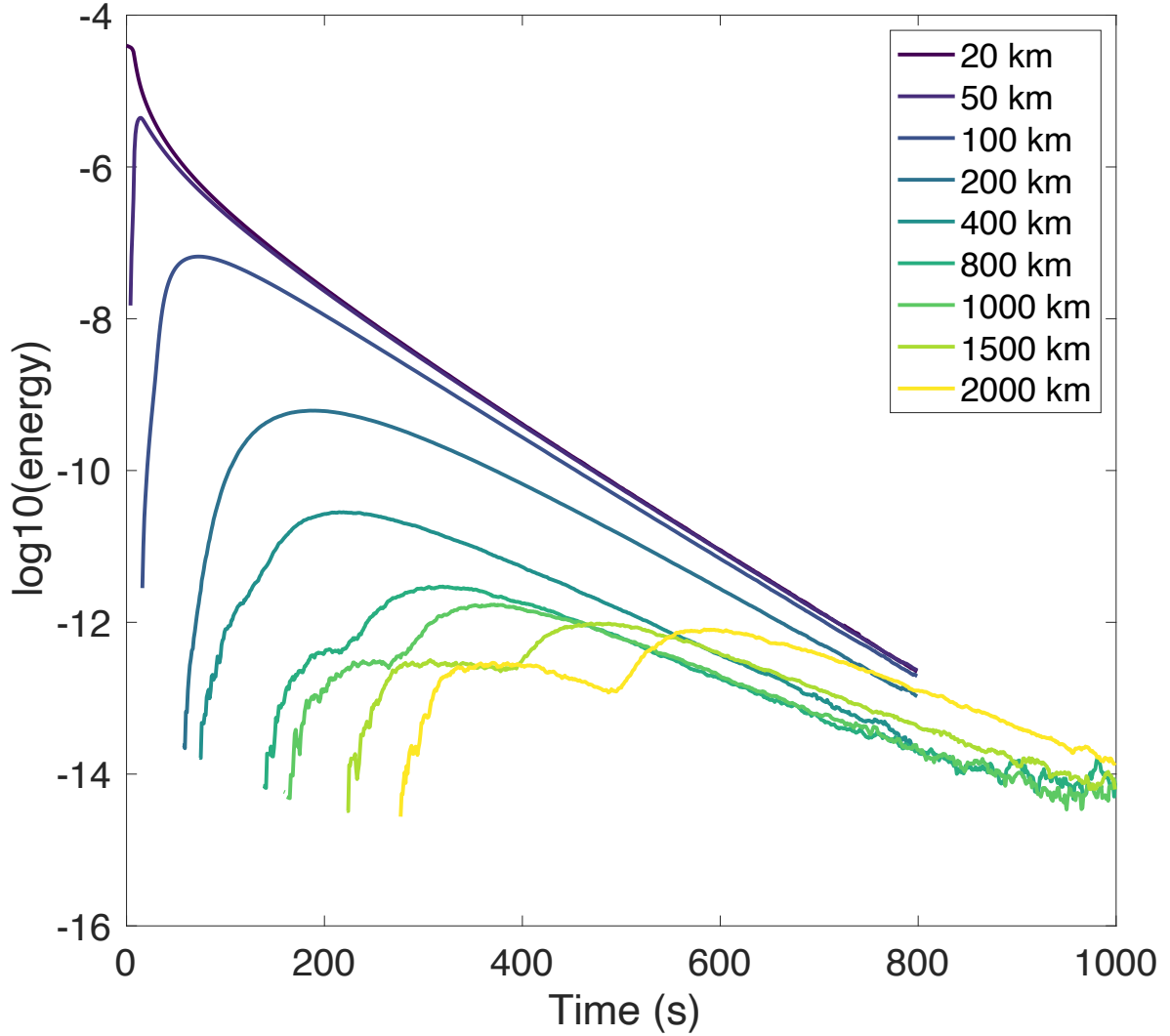


**Figure S4.** Synthetic coda evolution with diffusive subsurface structure. The calculation was made with 60km diffusive crust with  $Q_{scattering} = 56$  and  $Q_{\mu} = 2.35 \times 10^3$  overlying on a mantle with  $Q_{scattering} = 2.35 \times 10^{21}$  and  $Q_{\mu} = 2.35 \times 10^{21}$ . The model was chosen so that it well reproduces the observed coda evolution for VF type events. While the envelope shape change drastically at short distances, it shows moderate change after 200km distance.

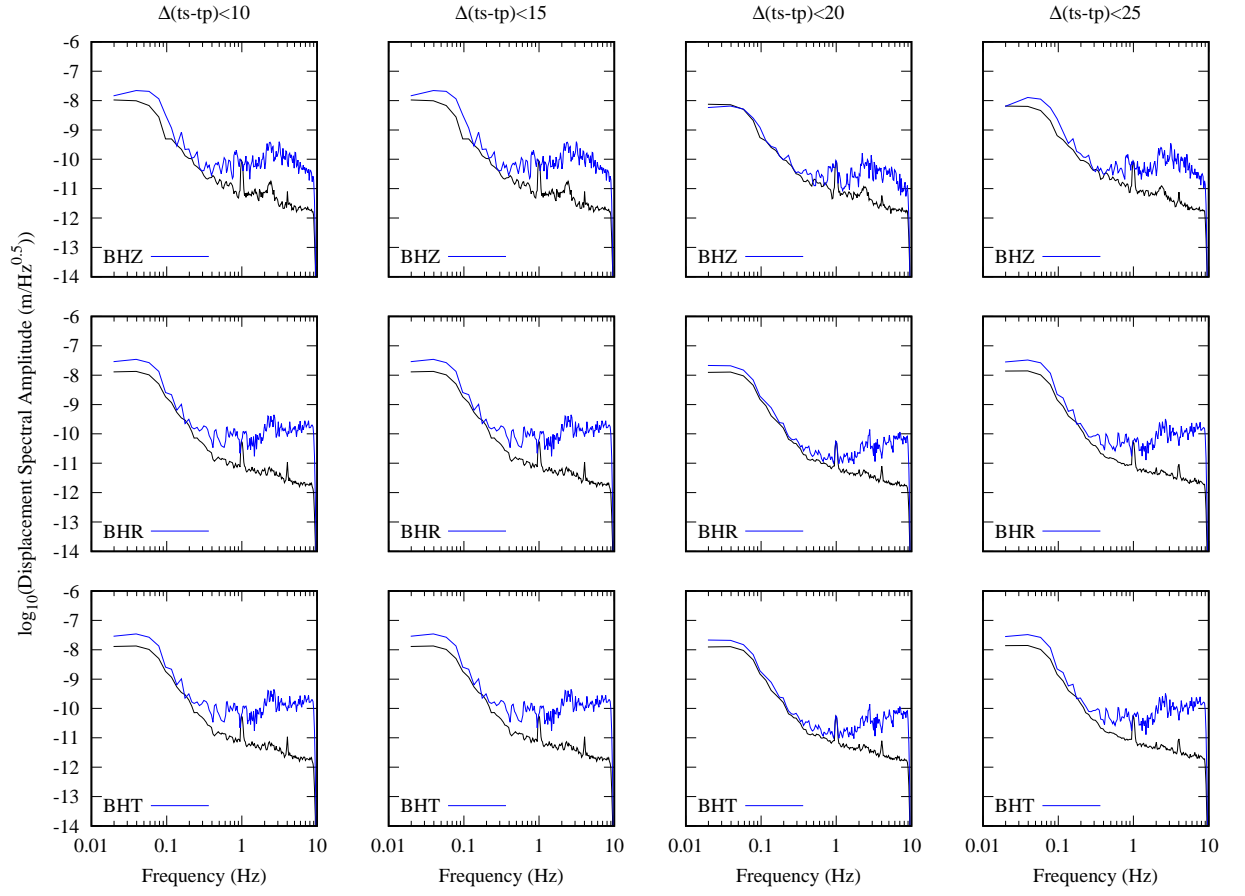


**Figure S5.** Comparison of EGFs calculated with different  $ts-tp$  margin ( $\Delta(ts-tp)$ ).  $\Delta(ts-tp)$  is defined as the difference that we accept for  $ts-tp$  time with respect to the reference value (i.e. S1222a:  $ts-tp=214s$ ). Each column shows the different  $\Delta(ts-tp)$  and each row shows the vertical, radial and transverse component. The blue lines show the EGFs and the black line is the stacked noise level. The difference is minor and we chose  $\Delta(ts-tp) = 25s$  to have larger number of events.

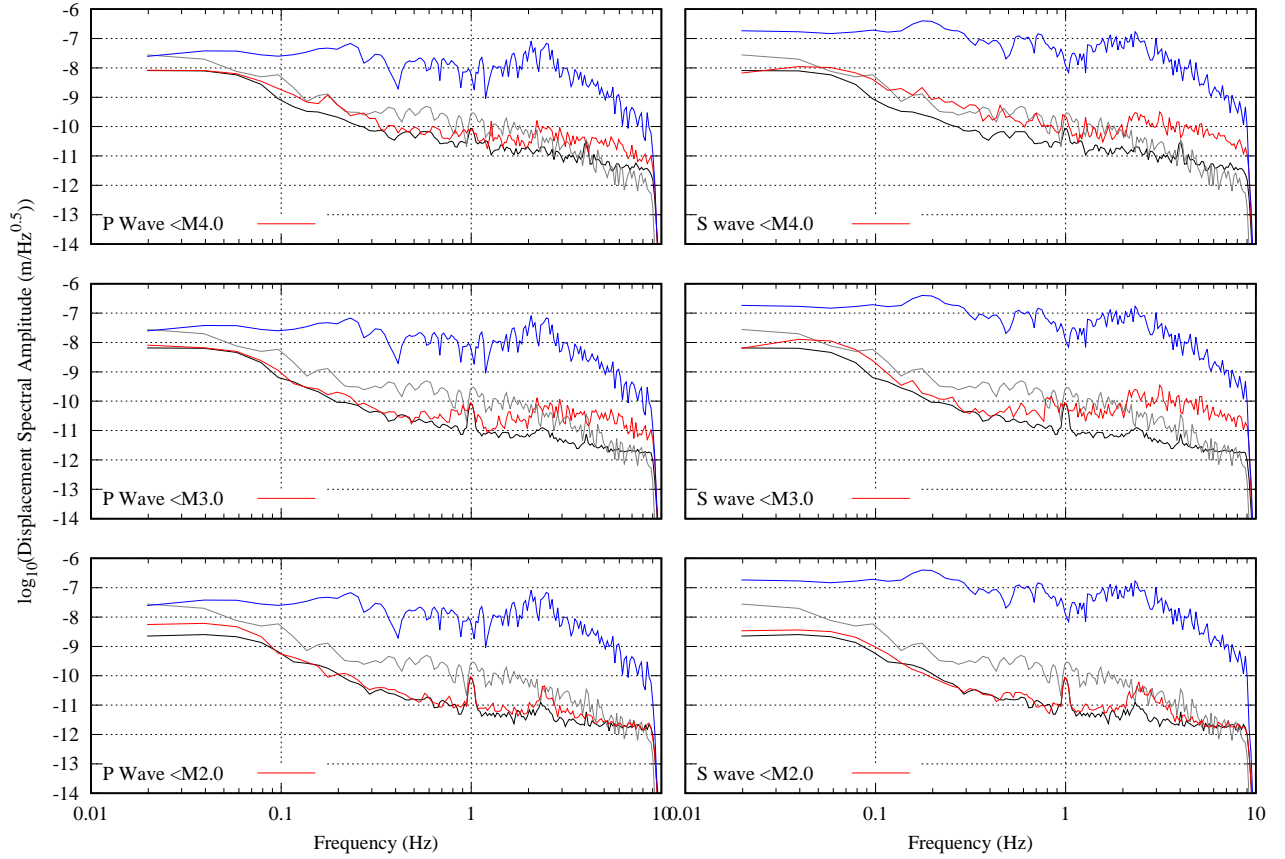


**Figure S6.** Comparison of EGFs calculated with different magnitude threshold. For each row we set the maximum magnitude to be included in the EGF estimation at  $M=2.0$ ,  $3.0$  and  $4.0$ . The left and right column show the P and S wave respectively. The red lines are the EGFs obtained and the black lines are the stacked noise. The blue lines are the spectra of S1222a and the gray lines are the noise spectra at the time of S1222a events. We found that when we take  $M=2.0$  as our threshold, the obtained EGFs have low S/N and they almost overlap with the noise except for the peak around  $2.4\text{Hz}$ . On the other hand, for  $M=3.0$  and  $4.0$ , we see the characteristic shape of the enhancement at the high frequency which well represents the contamination that we observed in the original data. Thus, we chose smaller value of  $M=3.0$  as our threshold to have smaller impact of corner frequencies of these events to the EGFs.



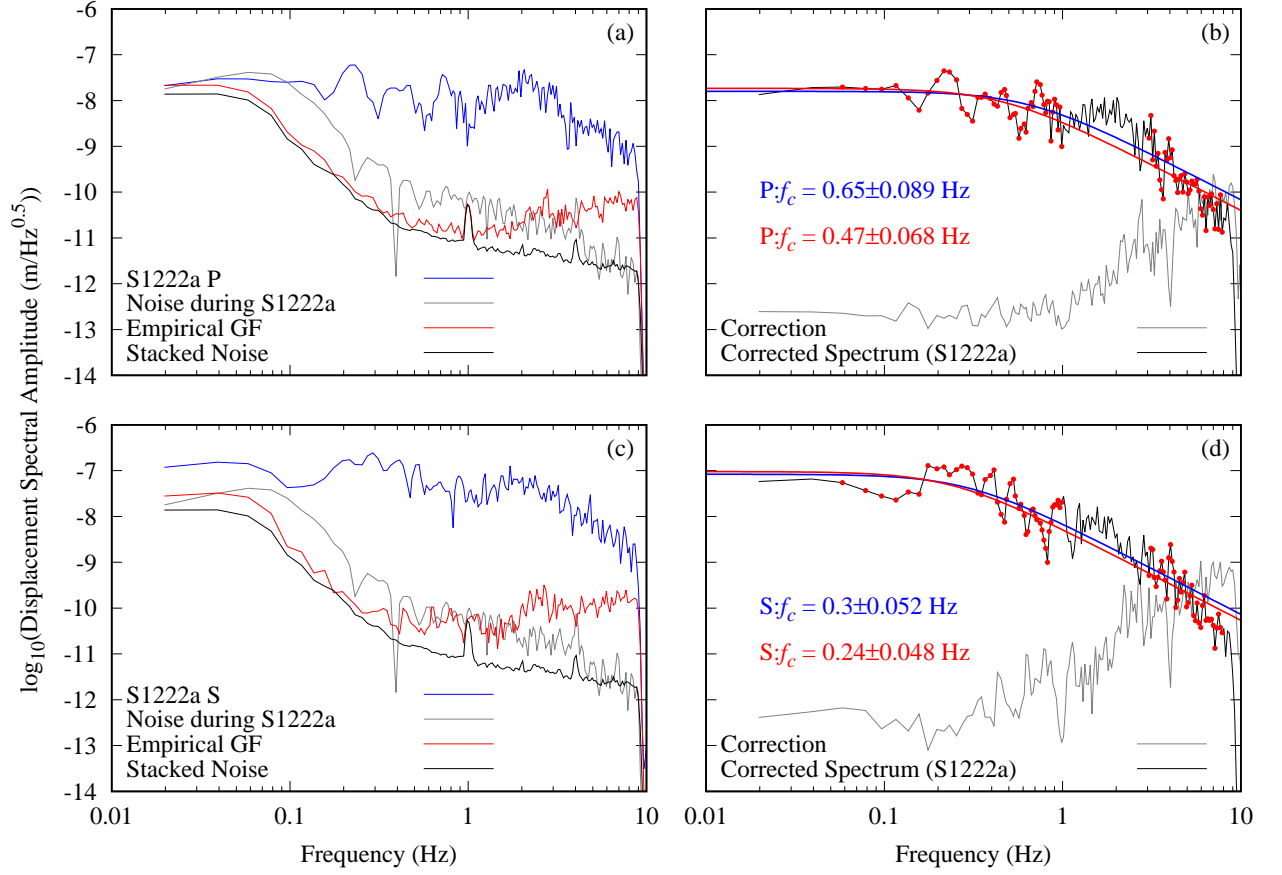


**Figure S7.** Empirical Green's Function (EGF) analyses performed for S1222a on the radial component. We used the same setting as Figure 3 in the main text. Note that since not all events have their back azimuth estimated from the data, we took both N and E component and stacked to obtain the EGF and the stacked noise

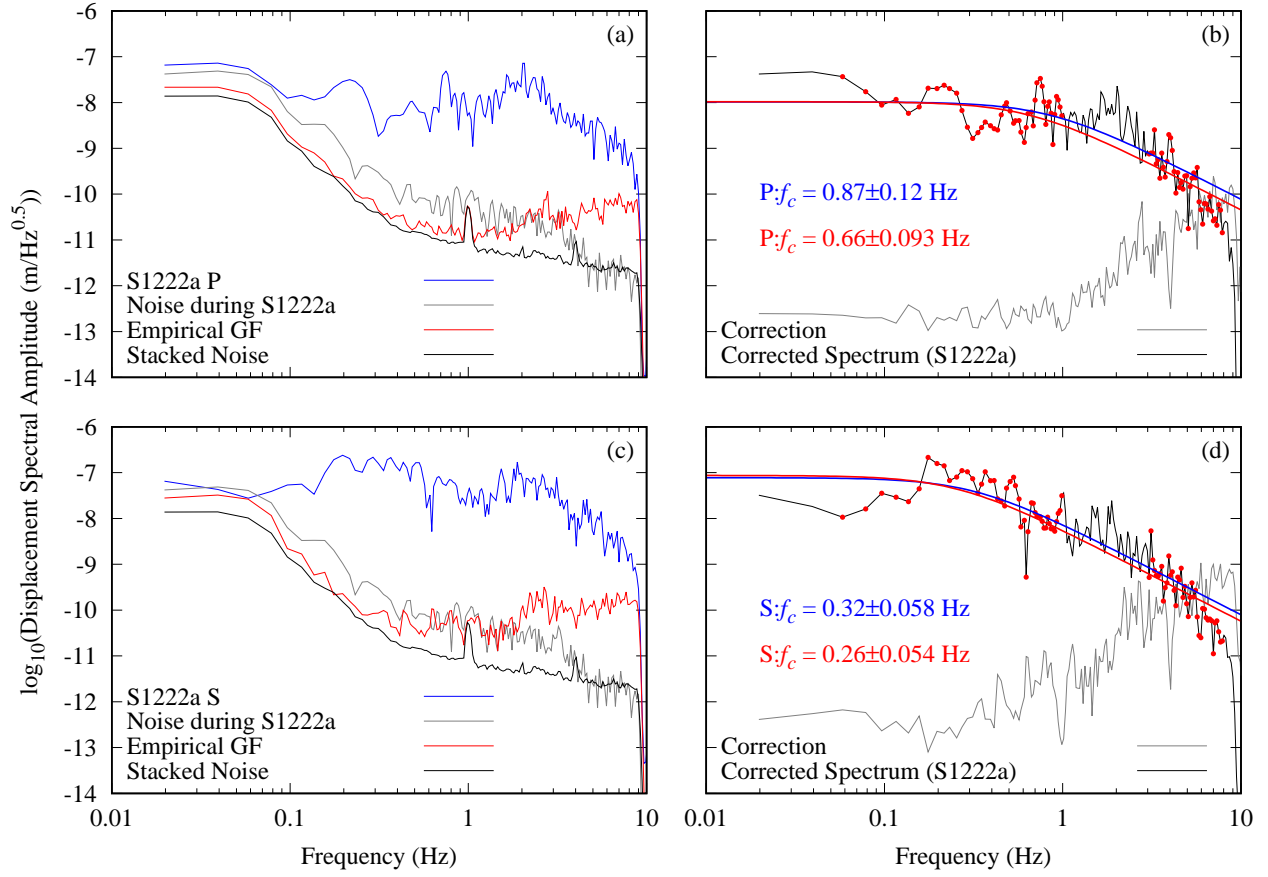


**Figure S8.** Empirical Green's Function (EGF) analyses performed for S1222a on the transverse component. We used the same setting as Figure 2 in the main text. Note that since not all events have their back azimuth estimated from the data, we took both N and E component and stacked to obtain the EGF and the stacked noise

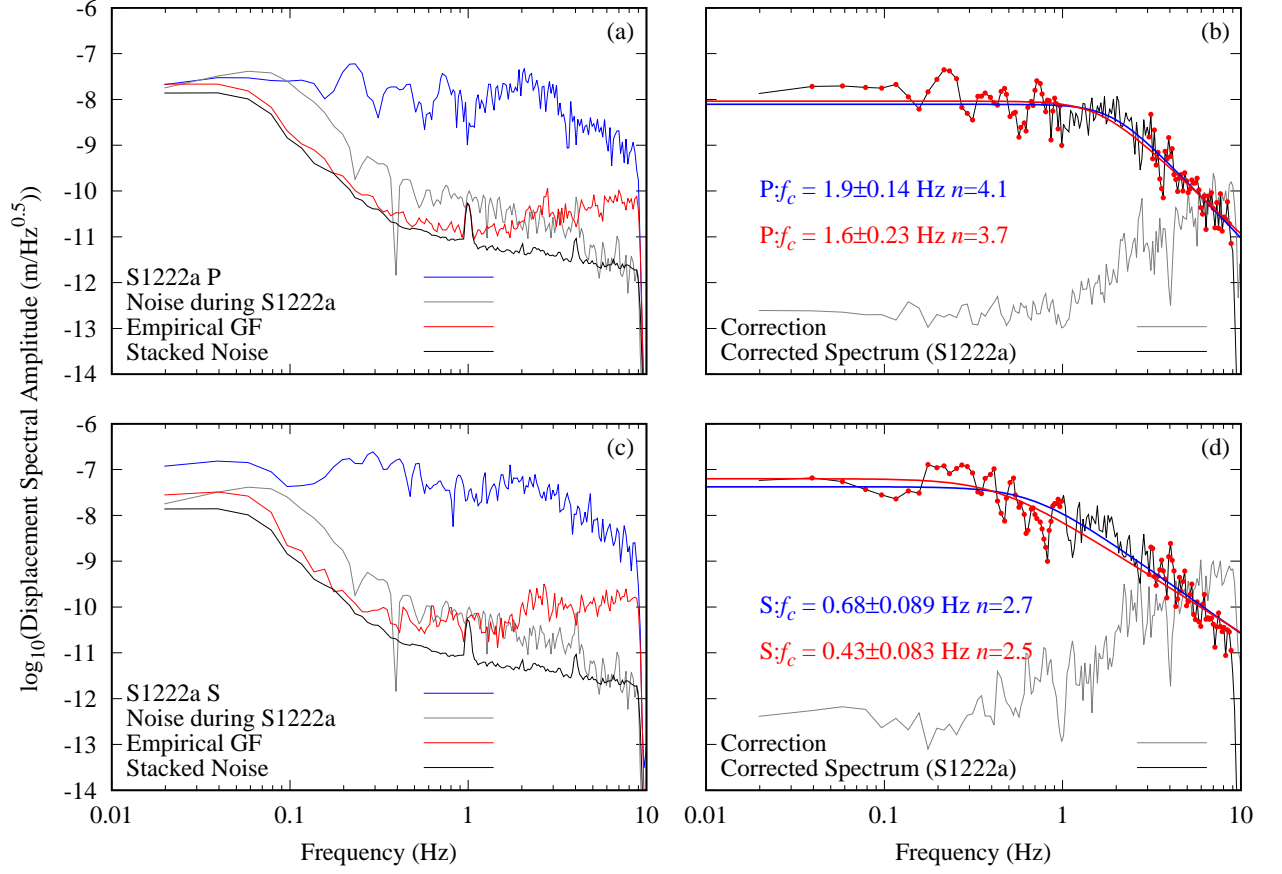


**Figure S9.** Empirical Green's Function (EGF) analyses performed for S1222a with general form of a source time function on radial component  $\gamma = 1$ . We used the same setting as Figure 2 in the main text. Note that since not all events have their back azimuth estimated from the data, we took both N and E component and stacked to obtain the EGF and the stacked noise.

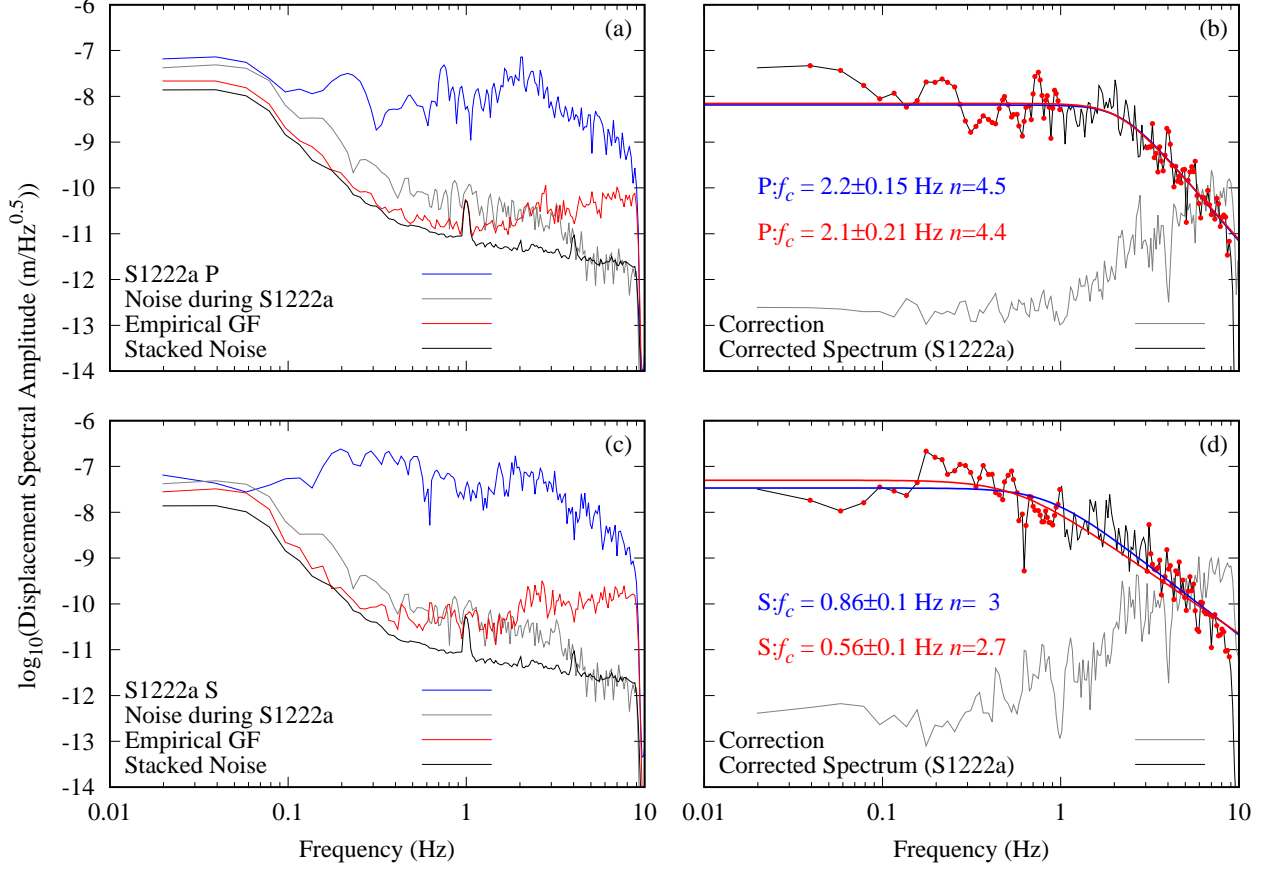


**Figure S10.** Empirical Green's Function (EGF) analyses performed for S1222a with general form of a source time function on transverse component  $\gamma = 1$ . We used the same setting as Figure 4 in the main text. Note that since not all events have their back azimuth estimated from the data, we took both N and E component and stacked to obtain the EGF and the stacked noise.

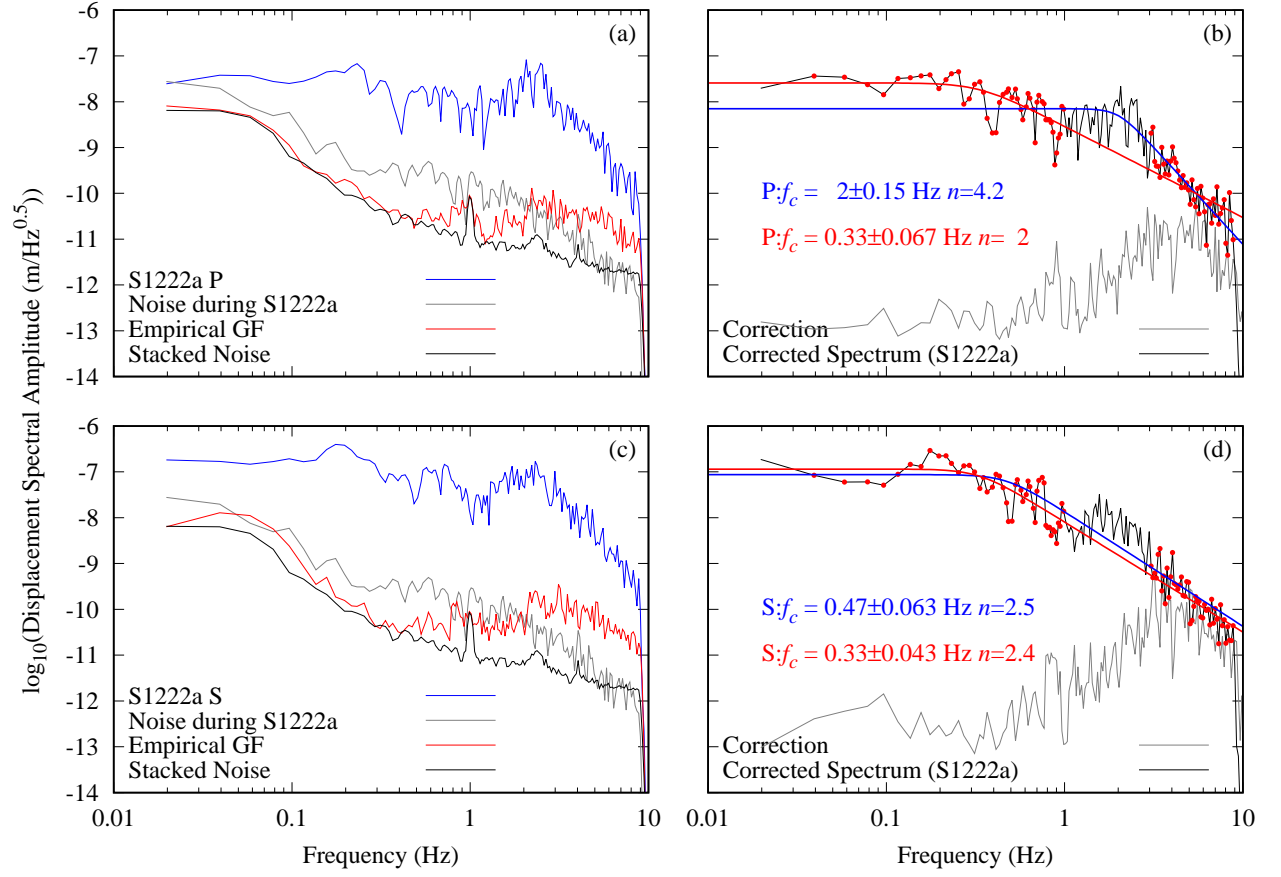


**Figure S11.** Empirical Green's Function (EGF) analyses performed for S1222a with general form of a source time function on vertical component  $\gamma = 2$ . We used the same setting as Figure 2 in the main text.

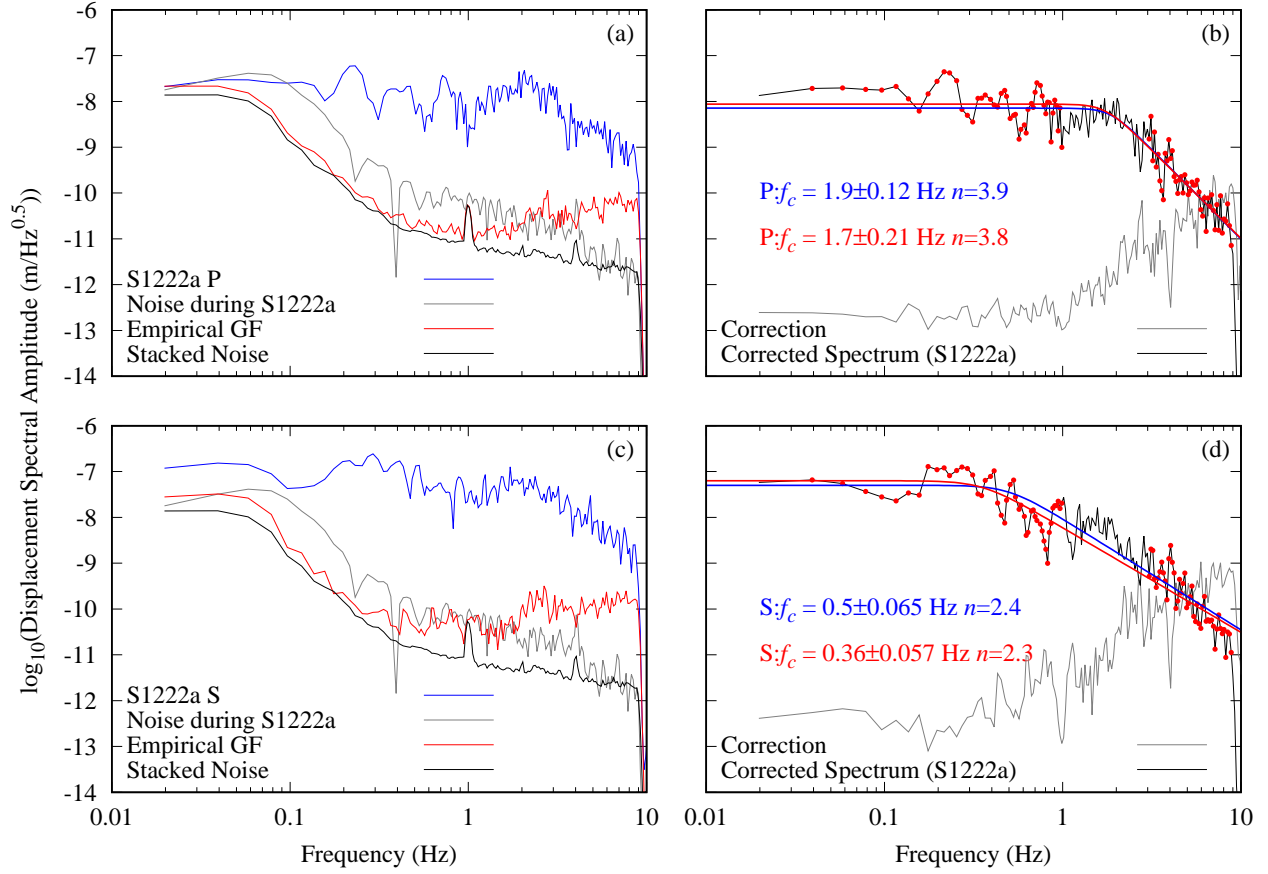


**Figure S12.** Empirical Green's Function (EGF) analyses performed for S1222a with general form of a source time function on radial component  $\gamma = 2$ . We used the same setting as Figure 2 in the main text. Note that since not all events have their back azimuth estimated from the data, we took both N and E component and stacked to obtain the EGF and the stacked noise.

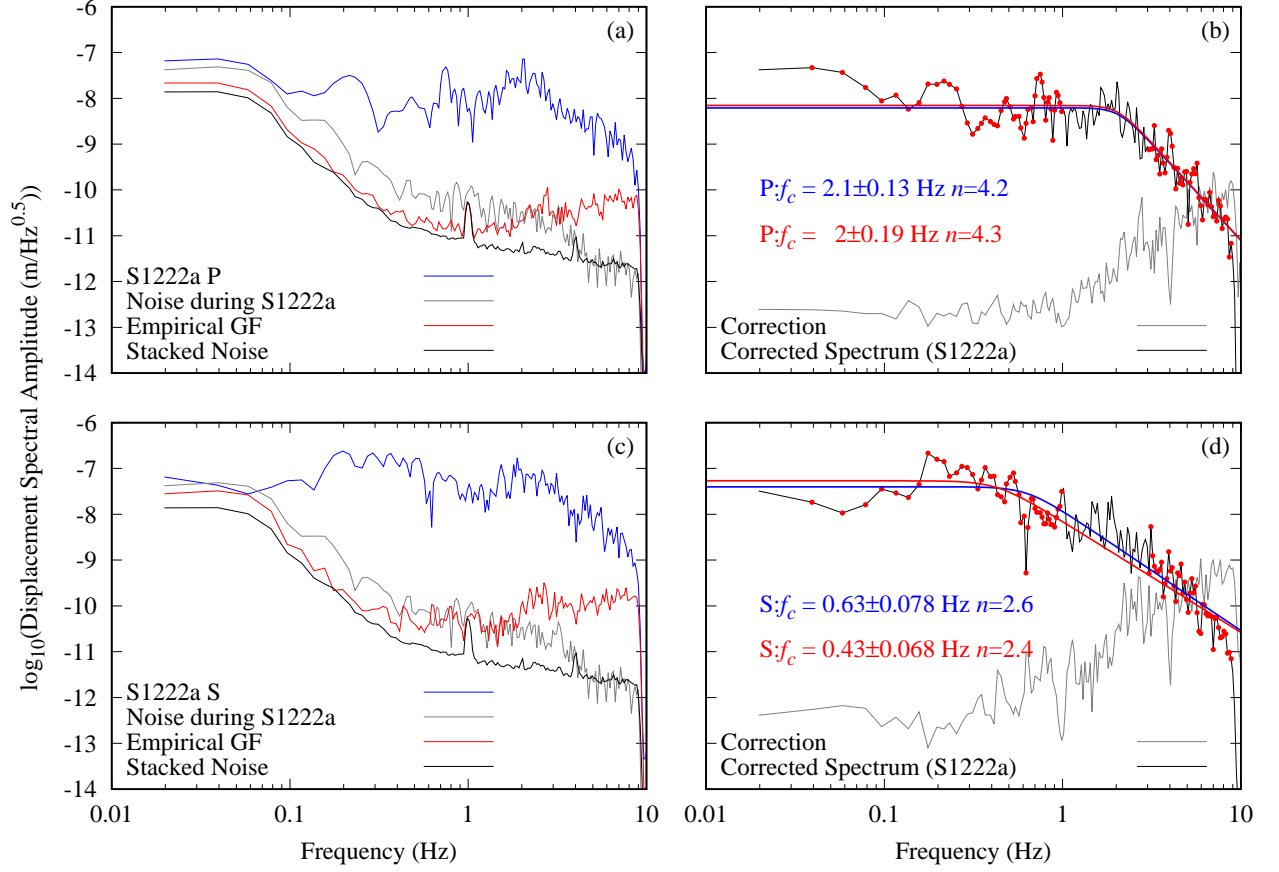


**Figure S13.** Empirical Green's Function (EGF) analyses performed for S1222a with general form of a source time function on transverse component  $\gamma = 2$ . We used the same setting as Figure 2 in the main text. Note that since not all events have their back azimuth estimated from the data, we took both N and E component and stacked to obtain the EGF and the stacked noise.